

**A Relation between Mass and Radius for 59 Exoplanets
with $R_{\text{P}} < 4R_{\oplus}$**

L. M. Weiss & G. W. Marcy

Received _____; accepted _____

We study the masses and radii of the 59 known exoplanets that have radii less than $4R_{\oplus}$. We find a linear relation of the form $M_P \approx 3R_P$. The RMS of planet masses is $3.8 M_{\oplus}$, and our best fit has reduced $\chi^2 = 3.4$, indicating a large diversity in planet compositions below $4R_{\oplus}$. Wu & Lithwick (2013), who also find $M_P \approx 3R_P$, note that the linear scaling is consistent with a constant escape velocity.

1. Introduction

The Kepler Mission has found an abundance of planets with $R < 4R_{\oplus}$ (Batalha et al. 2012). However, in many systems, it is difficult to measure the masses of such small planets because the gravitational acceleration these planets induce on their host stars or neighboring planets is too small to detect with current telescopes and instruments. How can we determine the composition of these planets?

Weiss et al. (2013) have shown that for planets between a few and thousands of Earth masses, we can predict the radius of a planet from its mass and incident stellar flux, suggesting that planets of a given mass have a particular composition. However, below $\sim 4 R_{\oplus}$, the large apparent scatter in planet mass makes predicting planet mass harder. At $2 R_{\oplus}$, planets are observed to span a decade in densities, from less dense than water to densities suggesting a solid iron composition.

There are two explanations for the large apparent scatter in planet densities: either errors in radius and/or mass measurements are underestimated for planets below $4 R_{\oplus}$, or the (real) scatter in radius indicates a diversity of planet compositions. Identifying whether this apparent variety in planet densities is real

or not is one of the most pressing issues in understanding planetary compositions today. Does the size of a planet uniquely determine a planet’s composition, or is there diversity of the rock, water, and H/He composition at a given mass? If the scatter is only apparent, then it is possible that there is a one-to-one correspondence between planet size and composition below $4 R_{\oplus}$. However, if the scatter is real, then there must be a diversity of planet compositions at a given mass below $4 R_{\oplus}$. Further refinements to the measurements of planet masses, especially below $4 R_{\oplus}$, are necessary to test to what extent the apparent scatter of planetary masses at a given radius is real.

Another way to probe the scatter in planet mass is to attempt to measure the masses of more small planets. Although uncertainties in the mass measurements for individual planets might be of order the planet mass, observing many small planets allows us to study the statistical distribution of planet masses for small planets. Marcy et al. (2013) have taken this approach to measure the masses of 42 small, transiting planets. This wealth of new data merits a reconsideration of the relation between planet mass and radius for small planets, which is the subject of this paper.

This updated examination of the mass-radius relation benefits from the masses and radii of 226 expo planets with $R_P < 4R_{\oplus}$. The sources of these measurements are (1) the masses of 42 planets with $R_P < 4R_{\oplus}$ from 22 stellar systems, characterized in Marcy et al. (2013), and (2) additional planets and/or refined stellar parameters for several systems, including 55 Cnc e (Endl et al. 2012)?, Kepler-11 (Lissauer et al. 2013), GJ 3470 (Demory et al. 2013), HD 97658 b (Dragomir et al. 2013), and KIC 8435766 (Sanchis-Ojeda et al. 2013)

A plot of radius versus mass for 226 exoplanets is shown in Figure 1. The planets are colored by incident flux from the host star; planets that receive more than the median flux (459 Earth fluxes) are red, while those that receive less are blue. Most of the planets that have been discovered since the publication of Weiss et al. (2013) are in the low-mass branch of this diagram. For this reason, and also because the relation between mass and radius for small planets is both poorly understood and vital for determining planet composition of small planets, we focus on the low-mass portion of the population. In the rest of this paper, we examine planets for which $R_P < 4R_\oplus$. We try to determine how their size correlates with their masses and densities (and therefore compositions), and we also investigate how other parameters might correlate with the physical properties of these small exoplanets.

2. Using Negative Planet Masses for Statistical Soundness

Marcy et al. (2013) allow “negative” planet masses as Keplerian orbital solutions to avoid the Lutz-Kelker bias. A “negative” planet mass arises when, given the orbital period and phase determined by the transit, the RV data have the opposite sign from what is expected. This yields a negative semi-amplitude K in the orbital solution, which results in a negative planet mass. See Marcy et al. (2013) for a more detailed discussion of this technique.

In a traditional analysis, the uncertainties in the RVs and the number of measurements combine to determine an upper limit to the planet mass. However, upper limits to planet masses are difficult to use statistically. The artifice of a

negative planet mass allows us to treat the population of small planets statistically. Since there is no bias toward large or small planet masses in our sample, we can take the weighted mean mass of planets of a given radius.

3. Justification for a Mass-Radius Relation for Small Exoplanets

Is there a correlation between planet mass and radius for small ($R_P < 4R_\oplus$) exoplanets? By eye, we might judge that there is a correlation, but what is the probability that we have fooled ourselves into believing there is a correlation when there is none?

To answer this question, we calculate the probability that mass and radius are uncorrelated. First, we calculate the correlation coefficient (Pearson R test) $r = 0.61$. There are 59 planets smaller than $4 R_\oplus$, leaving 57 degrees of freedom, so the Student t value is 5.75. The probability that these data are uncorrelated is 1.3×10^{-6} . Thus, the masses and radii of planets between the sizes of Earth and Neptune are correlated.

Another way to convince yourself that mass and radius are correlated for small planets is to examine Figure 2, which shows the weighted mean exoplanet mass in bins of width $1 R_\oplus$. On average, exoplanet mass increases with increasing radius, indicating an underlying correlation in the individual exoplanet masses and radii.

We conclude that for $R_P < 4R_\oplus$, exoplanet mass increases with increasing exoplanet radius.

4. The Updated Mass-Radius Relation for Small Exoplanets

Figure 3 suggests that exoplanet masses and radii can be fit with a line. We verify this with a traditional power-law fit and obtain $M_P \propto R_P$ as the best result.

The best linear fit to the data for $R_P < 4R_\oplus$ is:

$$M_P/M_\oplus = 0.2 + 2.6 R_P/R_\oplus$$

There are 59 exoplanets in this sample. The reduced $\chi^2 = 3.4$, and the RMS $= 3.8M_\oplus$.

To illustrate how this population of exoplanets compares to our Solar System, we plot the Solar System planets in Figure 3 as blue triangles. A quadratic fit to the exoplanet population happens to line up with the Solar System planets, but has a reduced χ^2 that is twice as large as the linear fit to the exoplanets. Since most of the exoplanets in this sample have $P < 50$ days, we do not expect them to behave the same way as Uranus and Neptune, which have orbital periods of tens of thousands of days. Therefore, the hefty masses of Uranus and Neptune compared to planets of similar size that are closer to their stars is not unreasonable. In fact, the difference in mass between Uranus and Neptune compared to closer-in planets of $4 R_\oplus$ distinguishes the quadratic fit as good for the solar system, as compared to the linear fit that is good for exoplanets.

5. Discussion

5.1. Interpretation of the Mass-Radius Relation

The correlation between exoplanet mass and radius for $R_P < 4R_\oplus$ indicates that Earth-size planets are less massive than Neptune-size planets.

The large reduced χ^2 values for the linear and quadratic mass-radius relations indicate that these relations are not sufficient models to explain the variation in planet mass at a given radius. Either a diversity of planet compositions, or correlation between the residuals and some other parameter, is required to explain the large scatter in planet mass.

The data are better described by a linear fit than a quadratic or cubic fit. Since a cubic fit of $M_P \propto R_P^3$ describes how mass and radius relate for constant density, a fit of $M_P \propto R_P$ indicates that planet density decreases strongly as mass or radius increases (see Figure 2 and 4). This can be attributed to an increasing fraction of volatiles with increasing planet mass.

Previous work, including Lissauer et al. (2011) and Weiss et al. (2013), suggest that the mass-radius relation is more like $M_P \propto R_P^2$ for small exoplanets. However, these studies include Saturn or Saturn-like planets at the high-mass end of their populations. Such planets might better be described as part of the giant planet population. Using the properties of Saturn-like planets in a relation that attempts to describe the properties of planets that are more like Earth and Neptune is misleading.

In a study of planets with $M_P < \sim 20M_\oplus$, Wu & Lithwick (2013) found

$M_P/M_\oplus \approx 3R_P/R_\oplus$ in a sample of 22 pairs of planets that exhibited strong anti-correlated transit timing variations (TTVs). Our independent assessment of 59 planets, 43 of which are newly reported and are not analyzed in Wu & Lithwick (2013), agrees with this result.

Wu & Lithwick (2013) noted that a linear relation between planet mass and radius is dimensionally consistent with a constant escape velocity from the planet (i.e. $v_{\text{esc}}^2 \sim M_P/R_P$). While this is one interpretation of the linear mass-radius relation for small exoplanets, there are perhaps other valid physical interpretations. For instance, a constant M_P/R_P implies that the gravitational potential energy $U \propto M_P/R_P$ of exoplanets is constant. This could be due to atmospheric particles escaping, but perhaps some other physical mechanism sets this energy level for exoplanets.

5.2. The Possible Role of Photoevaporation in Sculpting Small Planets

Strong stellar irradiation can either inflate a planet, as with hot Jupiters (Seager et al. 2007), or it can photoionize and strip the planet’s atmosphere, leaving a dense core (Lopez et al. 2012). Possible evidence for these processes can be seen in Figure 5, which shows that for massive planets ($M_P > 60M_\oplus$ or $R_P > 4R_\oplus$), high incident flux correlates with larger radius, whereas for low-mass planets ($M_P < 60M_\oplus$ or $R_P < 4R_\oplus$), high incident flux correlates with smaller radius.

Another way to describe how incident flux relates to exoplanet size is that for low levels of incident stellar flux (less than 100 times what Earth receives),

you can find planets ranging in size from Earth to Jupiter. However, at higher incident flux, there are only hot Earths (which might have been photo-evaporated) and hot Jupiters (which have been inflated). In other words, there are no hot Neptunes. Given the detection of hot and cold Earths, hot and cold Jupiters, and cold Neptunes, it seems unlikely that a detection bias causes the dearth of hot Neptunes; rather, their absence is likely astrophysical.

How significant is the decrease in planet size with increasing planet flux for small exoplanets? For $R_P < 4R_\oplus$, we find a correlation Pearson R coefficient between planet radius and incident stellar flux of $r = -0.19$. Over a sample of 71 planets, this corresponds to a Student-t value of $t = -1.6$, indicating a probability of 0.11 that these variables are uncorrelated. Repeating this calculation for a larger sample of exoplanets (for instance, the entire catalog of Kepler planets candidates, for which R_P and the incident flux on the planet are known) would reveal whether this correlation is real.

5.3. Correlation with Residuals

We examine the possibility that the residuals to the mass-radius fit correlate with some other parameter. The correlation between the residual (exoplanet mass minus predicted mass) and each of: the incident flux from the star, the semi-major axis, the orbital period, the stellar mass, and the stellar radius, all had magnitudes less than 0.1. The residuals as a function of orbital period, semi-major axis, and incident flux are shown in figure ???. For all of the parameters listed above, the probability that the residuals do not correlate with each parameter is at least 0.3

(i.e. mass residuals have at most a probability of 0.7 of correlating with one of the parameters listed above).

5.4. Interpretation of Planet Compositions

For detailed models of the compositions of the 42 new transiting planets presented in Marcy et al. (2013) and analyzed here, see Rogers (2013). Here, we consider the statistical properties of planet densities.

The densities of exoplanets with $R_P < 4R_\oplus$ are shown in Figure 4, and the densities binned by $1 R_\oplus$ are shown in Figure 2. Although the individual measurements of density for planets with $R_P < 2R_\oplus$ have large uncertainties (Figure 4), the weighted mean densities (Figure 2) for 0-1 R_\oplus and 1-2 R_\oplus show the continuation of the trend that smaller planets have higher densities. Figure 4 shows a dashed line at the density of Earth. Planets smaller than $2 R_\oplus$ tend to be denser than Earth, whereas planets larger than $2 R_\oplus$ tend to be less dense than Earth. However, since rock and other materials are compressible, planets that are as dense as Earth but have larger radii are not necessarily solid rock; they need some lighter materials, such as water or a H/He envelope, to achieve the density of Earth.

6. Conclusions

For exoplanets with $R_P < 4R_\oplus$ and $P < \sim 100$ days, planet radius correlates with planet mass. In this regime, the scaling between planet mass and radius is linear: $M_P/M_\oplus \approx 3R_P/R_\oplus$, indicating that larger planets have substantially more

volatiles than smaller planets. This relation is also different than what we observe for the Solar System planets smaller than Saturn, since Uranus and Neptune are more massive than the exoplanets of their size in this sample. A study of exoplanets of 3-4 R_{\oplus} with orbital periods of dozens of years would better contextualize Uranus and Neptune.

One reason Uranus and Neptune might be more massive than closer-in planets of the same size is that incident stellar flux might photo evaporate the atmospheres of closer-in counterparts, causing mass loss. The correlations between planet size and incident flux from the star for both large and small planets, and the absence of hot Neptunes, indicate that incident stellar flux of more than 100 times what Earth receives might play a key role in sculpting close-in planets.

Table 1. Exoplanets with Measured Mass and Radius and $R_P < 4R_\oplus$

Name	Planet Mass (M_\oplus)	Planet Radius (R_\oplus)	Incident Flux (F_\oplus)	Period (d)	First Ref.	Orbital Ref.
55 Cnc e	8.380	2.210	2439.690	0.737	McArthur et al. (2004)	Endl et al. (2012)
CoRoT-7 b	5.021	1.679	1779.433	0.854	Queloz et al. (2009); Léger et al. (2009)	Queloz et al. (2009)
CoRoT-8 b	68.673	6.389	88.184	6.212	Bordé et al. (2010)	Bordé et al. (2010)
GJ 1214 b	6.260	2.800	16.631	1.580	Charbonneau et al. (2009)	Carter et al. (2011)
GJ 3470 b	13.900	4.830	38.335	3.337	Bonfils et al. (2012)	Demory et al. (2013)
GJ 436 b	23.105	4.222	29.882	2.644	Butler et al. (2004)	Maness et al. (2007)
HAT-P-11 b	26.231	4.730	97.355	4.888	Bakos et al. (2010)	Bakos et al. (2010)
HAT-P-26 b	18.640	6.333	163.050	4.235	Hartman et al. (2011)	Hartman et al. (2011)
HD 97658 b	7.862	2.340	48.052	9.491	Howard et al. (2011)	Dragomir et al. (2013)
Kepler-10 b	4.539	1.416	3572.048	0.837	Batalha et al. (2011)	Batalha et al. (2011)
Kepler-11 b	1.900	1.800	126.384	10.304	Lissauer et al. (2011)	Lissauer et al. (2013)
Kepler-11 c	2.900	2.870	91.413	13.025	Lissauer et al. (2011)	Lissauer et al. (2011)
Kepler-11 d	7.300	3.120	43.562	22.687	Lissauer et al. (2011)	Lissauer et al. (2011)
Kepler-11 e	8.000	4.190	27.524	31.996	Lissauer et al. (2011)	Lissauer et al. (2011)
Kepler-11 f	2.000	2.490	16.745	46.689	Lissauer et al. (2011)	Lissauer et al. (2011)
Kepler-18 b	6.900	2.000	462.244	3.505	Borucki et al. (2011)	Cochran et al. (2011)
Kepler-18 c	17.299	5.490	163.493	7.642	Borucki et al. (2011)	Cochran et al. (2011)
Kepler-18 d	16.399	6.980	67.364	14.859	Borucki et al. (2011)	Cochran et al. (2011)
Kepler-20 b	8.474	1.908	343.928	3.696	Borucki et al. (2011)	Gautier et al. (2012)
Kepler-20 c	15.734	3.067	81.783	10.854	Borucki et al. (2011)	Gautier et al. (2012)
Kepler-20 d	7.528	2.748	5.937	77.612	Borucki et al. (2011)	Gautier et al. (2012)
Kepler-36 b	4.461	1.485	217.365	13.840	Borucki et al. (2011)	Carter et al. (2012)
Kepler-36 c	8.101	3.676	175.646	16.239	Carter et al. (2012)	Carter et al. (2012)
Kepler-4 b	24.544	4.002	1123.918	3.213	Borucki et al. (2010)	Borucki et al. (2010)
Kepler-68 b	8.300	2.310	409.092	5.399	Borucki et al. (2011)	Gilliland et al. (2013)
Kepler-68 c	4.377	0.952	189.764	9.605	Batalha et al. (2013)	Gilliland et al. (2013)
KOI-94 b	9.400	1.770	1155.374	3.743	Weiss et al. (2013)	Weiss et al. (2013)
KOI-94 c	8.300	4.280	295.035	10.424	Borucki et al. (2011)	Weiss et al. (2013)
KOI-94 d	105.000	11.400	106.760	22.343	Borucki et al. (2011)	Weiss et al. (2013)
KOI-94 e	38.000	6.640	32.631	54.320	Borucki et al. (2011)	Weiss et al. (2013)
KOI-41.01	0.85000000	2.2000000	1156.6217	12.815900	Borucki et al. (2011)	Marcy et al. (2013)
KOI-41.02	7.3400000	1.3000000	65.166782	6.8870500	Borucki et al. (2011)	Marcy et al. (2013)
KOI-41.03	-5.3100000	1.6000000	85.869041	35.333100	Borucki et al. (2011)	Marcy et al. (2013)
KOI-69.01	2.5900000	1.5000000	172.33078	4.7267400	Borucki et al. (2011)	Marcy et al. (2013)
KOI-82.01	8.9300000	2.2000000	806.96474	16.145700	Borucki et al. (2011)	Marcy et al. (2013)
KOI-82.02	3.8000000	1.2000000	147.34753	10.311700	Borucki et al. (2011)	Marcy et al. (2013)
KOI-82.03	8.1200000	0.90000000	447.82440	27.453600	Borucki et al. (2011)	Marcy et al. (2013)
KOI-82.04	-2.4500000	0.60000000	447.27347	7.0714200	Borucki et al. (2011)	Marcy et al. (2013)
KOI-82.05	0.41000000	0.50000000	2950.4414	5.2869600	Borucki et al. (2011)	Marcy et al. (2013)
KOI-104.01	10.840000	3.5000000	1189.7862	2.5080600	Borucki et al. (2011)	Marcy et al. (2013)
KOI-108.01	18.690000	3.4000000	348.15857	15.965400	Borucki et al. (2011)	Marcy et al. (2013)

Table 1—Continued

Name	Planet Mass (M_{\oplus})	Planet Radius (R_{\oplus})	Incident Flux (F_{\oplus})	Period (d)	First Ref.	Orbital Ref.
KOI-108.02	-22.540000	5.1000000	163.05049	179.61200	Borucki et al. (2011)	Marcy et al. (2013)
KOI-116.01	10.440000	2.5000000	308.73816	13.570800	Borucki et al. (2011)	Marcy et al. (2013)
KOI-116.02	11.170000	2.6000000	604.88523	43.844500	Borucki et al. (2011)	Marcy et al. (2013)
KOI-116.03	0.15000000	0.80000000	416.85849	6.1648600	Borucki et al. (2011)	Marcy et al. (2013)
KOI-116.04	-13.340000	0.90000000	298.50217	23.980200	Borucki et al. (2011)	Marcy et al. (2013)
KOI-122.01	13.000000	3.4000000	1191.9507	11.523100	Borucki et al. (2011)	Marcy et al. (2013)
KOI-123.01	1.3000000	2.4000000	618.50330	6.4816300	Borucki et al. (2011)	Marcy et al. (2013)
KOI-123.02	2.2200000	2.5000000	1914.9410	21.222700	Borucki et al. (2011)	Marcy et al. (2013)
KOI-148.01	3.9400000	1.9000000	1903.1669	4.7780000	Borucki et al. (2011)	Marcy et al. (2013)
KOI-148.02	14.610000	2.7000000	537.46087	9.6739500	Borucki et al. (2011)	Marcy et al. (2013)
KOI-148.03	7.9300000	2.0000000	1030.1836	42.896100	Borucki et al. (2011)	Marcy et al. (2013)
KOI-153.01	-5.7000000	2.2000000	1818.3791	8.9250700	Borucki et al. (2011)	Marcy et al. (2013)
KOI-153.02	7.1000000	1.8000000	439.71133	4.7540000	Borucki et al. (2011)	Marcy et al. (2013)
KOI-244.01	24.600000	5.2000000	226.04191	12.720400	Borucki et al. (2011)	Marcy et al. (2013)
KOI-244.02	9.6000000	2.7000000	1560.3683	6.2385000	Borucki et al. (2011)	Marcy et al. (2013)
KOI-245.01	-5.9800000	1.9000000	1367.9423	39.792200	Borucki et al. (2011)	Marcy et al. (2013)
KOI-245.02	3.3500000	0.80000000	1611.6302	21.302000	Borucki et al. (2011)	Marcy et al. (2013)
KOI-245.03	-0.42000000	0.30000000	2337.2286	13.367500	Borucki et al. (2011)	Marcy et al. (2013)
KOI-246.01	7.8900000	2.3000000	926.85884	5.3987500	Borucki et al. (2011)	Marcy et al. (2013)
KOI-246.02	2.1800000	1.0000000	1299.0590	9.6050400	Borucki et al. (2011)	Marcy et al. (2013)
KOI-261.01	8.4600000	2.7000000	4070.4875	16.238500	Borucki et al. (2011)	Marcy et al. (2013)
KOI-283.01	16.130000	2.4000000	1637.1673	16.092000	Borucki et al. (2011)	Marcy et al. (2013)
KOI-283.02	17.020000	0.80000000	909.50346	25.516900	Borucki et al. (2011)	Marcy et al. (2013)
KOI-292.01	3.5100000	1.5000000	584.57028	2.5866400	Borucki et al. (2011)	Marcy et al. (2013)
KOI-299.01	3.5500000	2.0000000	1299.4980	1.5416800	Borucki et al. (2011)	Marcy et al. (2013)
KOI-305.01	6.1500000	1.5000000	142.83632	4.6035800	Borucki et al. (2011)	Marcy et al. (2013)
KOI-321.01	6.3500000	1.4000000	344.40060	2.4262900	Borucki et al. (2011)	Marcy et al. (2013)
KOI-321.02	2.7100000	0.80000000	725.85388	4.6233200	Borucki et al. (2011)	Marcy et al. (2013)
KOI-1442.01	0.060000000	1.1000000	11.621547	0.66931000	Borucki et al. (2011)	Marcy et al. (2013)
KOI-1612.01	0.48000000	0.80000000	1420.2428	2.4650200	Borucki et al. (2011)	Marcy et al. (2013)
KOI-1925.01	2.6900000	1.2000000	418.26336	68.958400	Borucki et al. (2011)	Marcy et al. (2013)
KIC 8435766	1.59	0.98	3093.3884	0.35500744	Sanchis-Ojeda et al. (2013)	Sanchis-Ojeda et al. (2013)

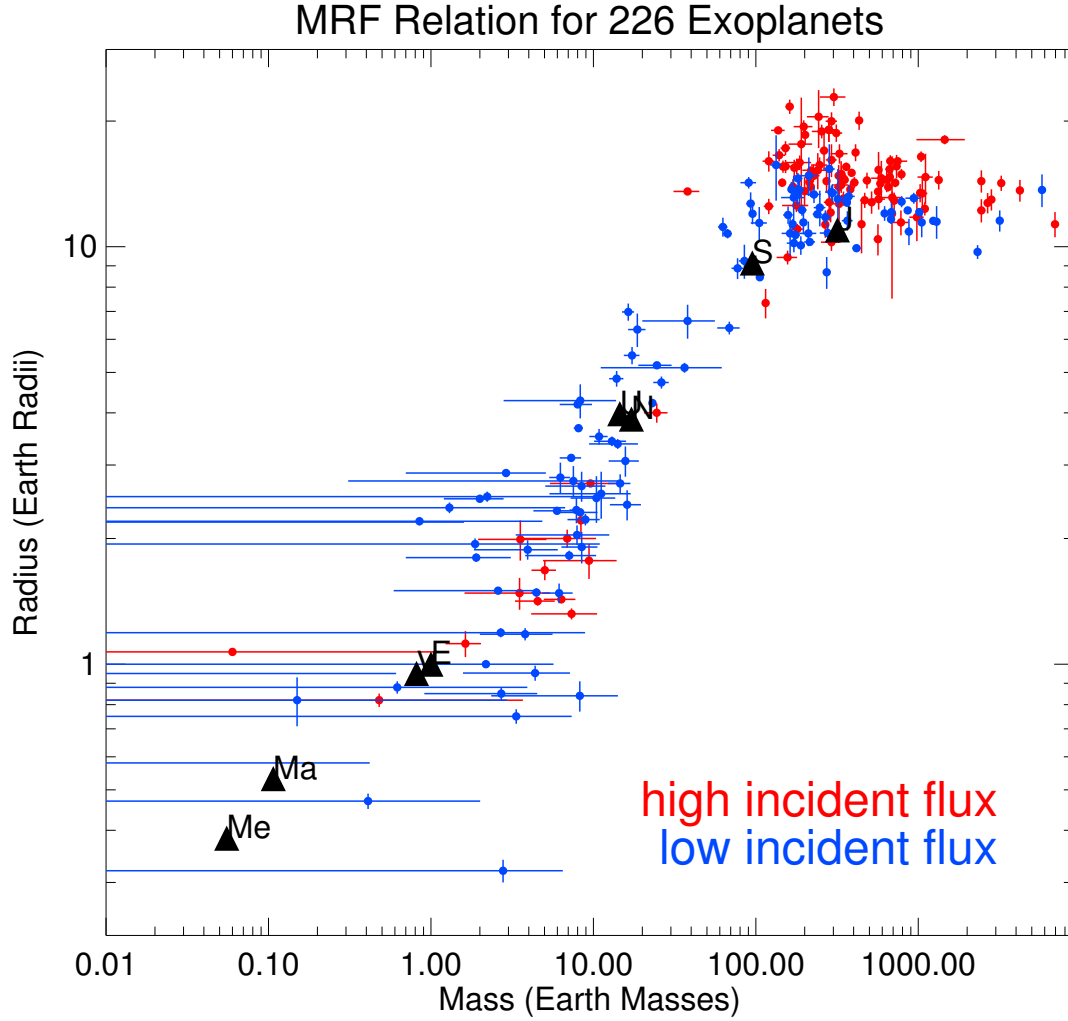


Fig. 1.— Radius vs. mass for exoplanets with measured masses and radii. Planets receiving lower than the median incident flux from this sample (459 times the incident flux at Earth) are blue; those receiving higher than the median incident flux are red. The Solar System planets are over plotted as black triangles for comparison. For giant planets ($M_P \geq \frac{1}{2}M_{\text{Sat}}$), planet radius correlates with incident flux, whereas for the smaller planets, radius and incident flux appear anti-correlated (see Figure 5).

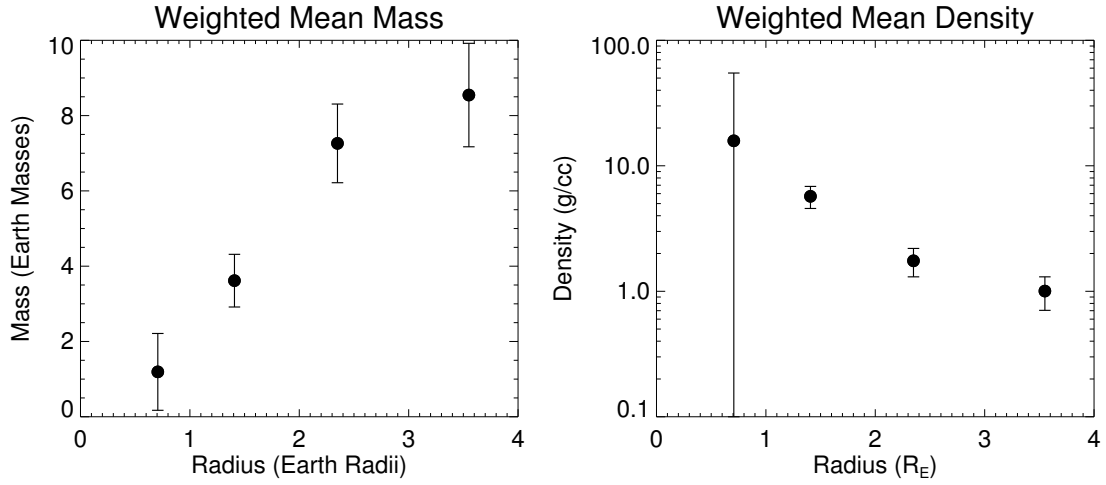


Fig. 2.— The weighted mean mass (left) and density (right) for exoplanets with $R_P < 4R_{\oplus}$ in bins of $1 R_{\oplus}$. The error bars are the weighted uncertainties in the means. Larger exoplanet radii correlate with larger masses but lower densities, indicating that large planets have a larger mass fraction of volatiles than small planets.

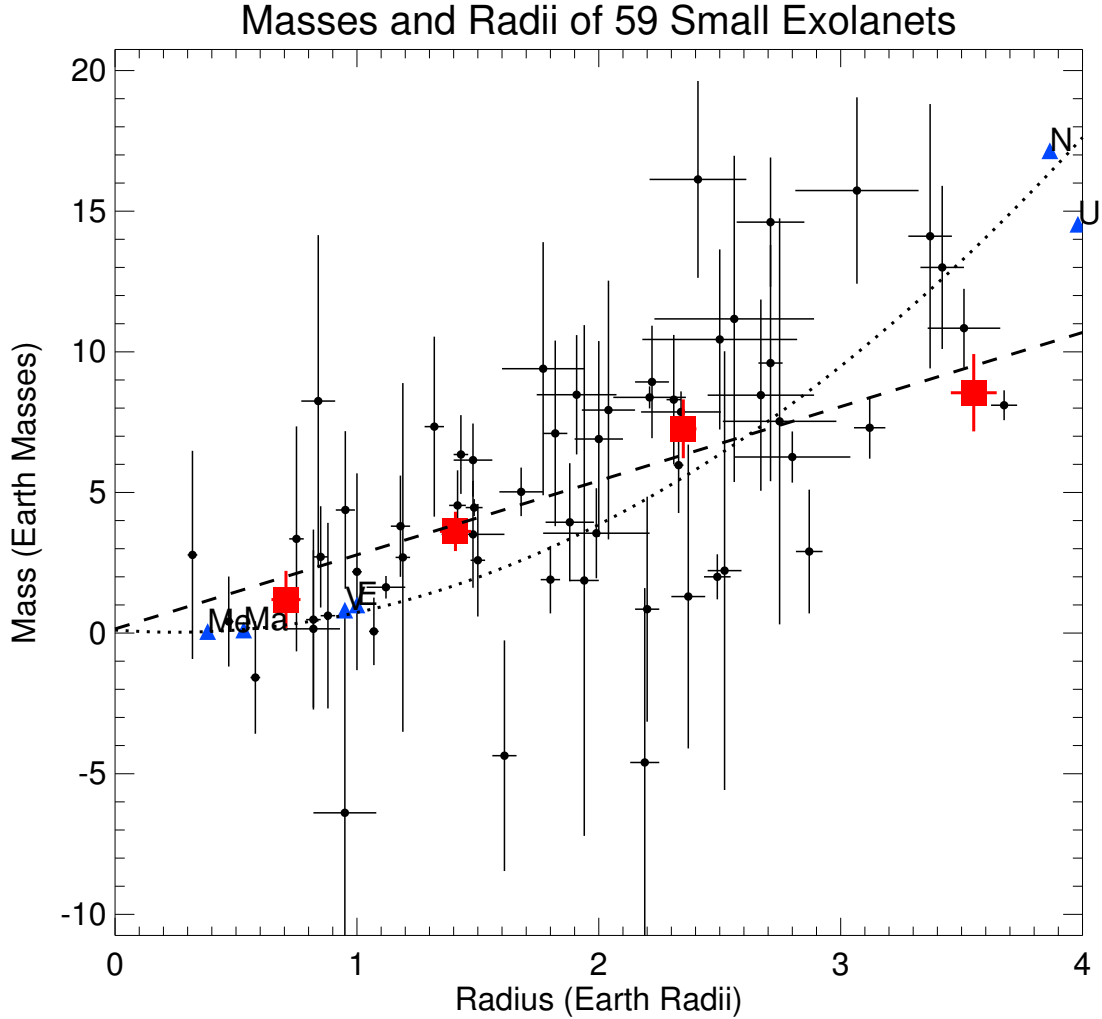


Fig. 3.— Mass vs. radius for 59 planets with $R_P < 4R_\oplus$ and 1σ uncertainties. The dashed line is the best linear fit to the 59 exoplanets: $M_P/M_\oplus = 0.2 + 2.6 \times R_P/R_\oplus$, $\chi^2/\nu = 3.4$. The dotted line is the best quadratic fit to the 59 exoplanets and 6 Solar System planets: $M_P = 0.1 - 0.6R_P + 1.25R_P^2$, in which we assumed errors in M_P and R_P for S.S. planets were 10^{-5} of their values. Red squares represent the weighted mean mass in bins of $1 R_\oplus$, and error bars are the uncertainty in the mean mass (as in Figure 2), to guide the eye. Note that a linear fit goes through the the weighted mean of the exoplanet population). The solar system planets are plotted as blue triangles. Note that Uranus and Neptune are much colder than the exoplanets in this sample.

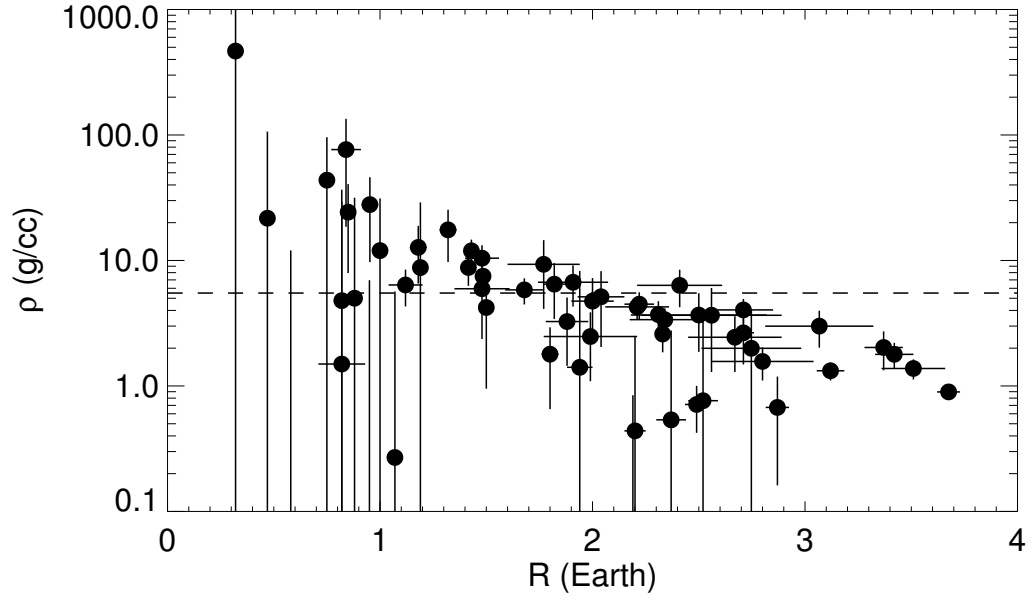


Fig. 4.— Density vs. radius for planets with $R_P < 4R_{\oplus}$ and 1σ uncertainties. Smaller planets are denser than larger planets. For reference, the density of Earth (5.5 g cm^{-3}) is shown as a dashed line.

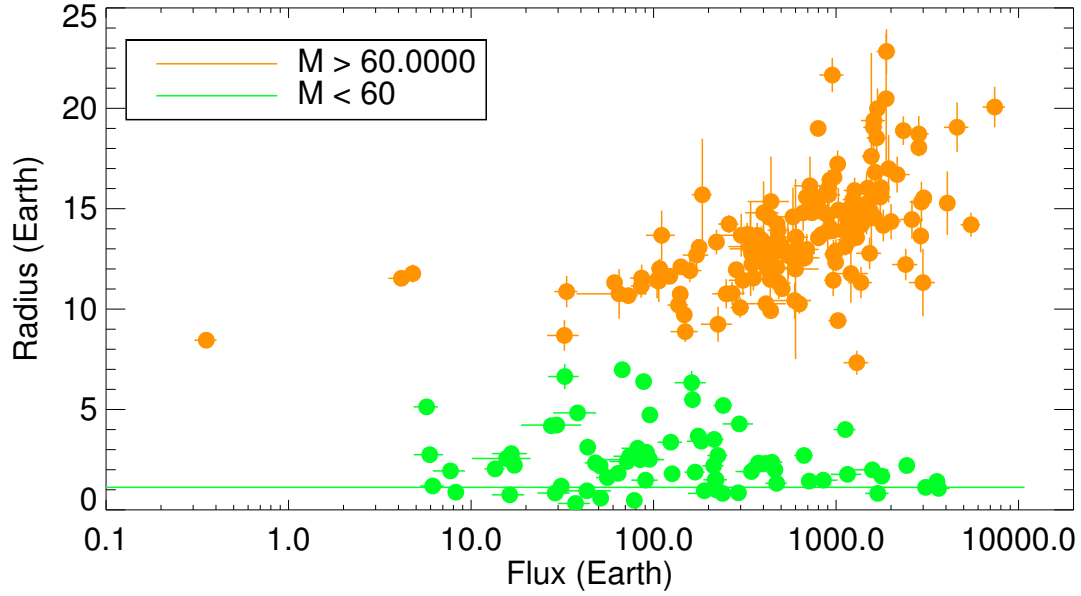


Fig. 5.— Radius vs. flux and 1σ uncertainties for exoplanets with measured masses and radii. Giant planets are orange; low-mass planets are green. For giant planets, radius increases with increasing incident flux from the star; for small planets, radius slightly decreases with increasing flux, especially above a few hundred Earth fluxes. There are no hot Neptunes. Note that all the planets with $R_P < 4R_\oplus$ are in the low-mass population.

REFERENCES

- Bakos, G. Á., Torres, G., Pál, A., et al. 2010, *ApJ*, 710, 1724
- Batalha, N. M., Borucki, W. J., Bryson, S. T., et al. 2011, *ApJ*, 729, 27
- Batalha, N. M., Rowe, J. F., Bryson, S. T., et al. 2012, *ArXiv e-prints*
- . 2013, *ApJS*, 204, 24
- Bonfils, X., Gillon, M., Udry, S., et al. 2012, *A&A*, 546, A27
- Bordé, P., Bouchy, F., Deleuil, M., et al. 2010, *A&A*, 520, A66
- Borucki, W. J., Koch, D. G., Brown, T. M., et al. 2010, *ApJ*, 713, L126
- Borucki, W. J., Koch, D. G., Basri, G., et al. 2011, *ApJ*, 736, 19
- Butler, R. P., Vogt, S. S., Marcy, G. W., et al. 2004, *ApJ*, 617, 580
- Carter, J. A., Winn, J. N., Holman, M. J., et al. 2011, *ApJ*, 730, 82
- Carter, J. A., Agol, E., Chaplin, W. J., et al. 2012, *Science*, 337, 556
- Charbonneau, D., Berta, Z. K., Irwin, J., et al. 2009, *Nature*, 462, 891
- Cochran, W. D., Fabrycky, D. C., Torres, G., et al. 2011, *ApJS*, 197, 7
- Demory, B.-O., Torres, G., Neves, V., et al. 2013, *ApJ*, 768, 154
- Dragomir, D., Matthews, J. M., Eastman, J. D., et al. 2013, *ApJ*, 772, L2
- Endl, M., Robertson, P., Cochran, W. D., et al. 2012, *ApJ*, 759, 19

- Gautier, III, T. N., Charbonneau, D., Rowe, J. F., et al. 2012, *ApJ*, 749, 15
- Gilliland, R. L., Marcy, G. W., Rowe, J. F., et al. 2013, *ApJ*, 766, 40
- Hartman, J. D., Bakos, G. Á., Kipping, D. M., et al. 2011, *ApJ*, 728, 138
- Howard, A. W., Johnson, J. A., Marcy, G. W., et al. 2011, *The Astrophysical Journal*, 726, 73
- Léger, A., Rouan, D., Schneider, J., et al. 2009, *A&A*, 506, 287
- Lissauer, J. J., Fabrycky, D. C., Ford, E. B., et al. 2011, *Nature*, 470, 53
- Lissauer, J. J., Jontof-Hutter, D., Rowe, J. F., et al. 2013, *ApJ*, 770, 131
- Lopez, E. D., Fortney, J. J., & Miller, N. K. 2012, *ArXiv e-prints*
- Maness, H. L., Marcy, G. W., Ford, E. B., et al. 2007, *PASP*, 119, 90
- Marcy, G. W., Isaacson, H., & Rowe, J. F. 2013, in prep.
- McArthur, B. E., Endl, M., Cochran, W. D., et al. 2004, *ApJ*, 614, L81
- Queloz, D., Bouchy, F., Moutou, C., et al. 2009, *A&A*, 506, 303
- Rogers, L. 2013, in prep.
- Sanchis-Ojeda, R., Rappaport, S., Winn, J. N., et al. 2013, *ApJ*, 774, 54
- Seager, S., Kuchner, M., Hier-Majumder, C. A., & Militzer, B. 2007, *ApJ*, 669, 1279
- Weiss, L. M., Marcy, G. W., Rowe, J. F., et al. 2013, *ApJ*, 768, 14
- Wu, Y., & Lithwick, Y. 2013, *ApJ*, 772, 74

